Three-Dimensional One Strut Failure Soil-structure Interaction Analysis for Strutted Diaphragm Wall Design by a New Mathematical Model - Two-Dimensional Plane Strain Finite Element Analysis combined with Plate Bending Theory

Raymond W. M. Lo[1], BSc, MSc, MHKIE, MIStructE, CEng and Daniel S.M. Bali[2], BSc, MSc.

[1]Senior Geotechnical Engineer, Aurecon New Zealand Limited, 139 Carlton Gore Road, Newmarket, Auckland, New Zealand- PH (064) 09-5238640; FAX (064) 09-5247815; email: Raymond.Lo@aurecongroup.com
[2]Geotechnical Engineer, Aurecon Singapore (Pte.) Ltd., 152 Beach Road #22-02, Gateway East, Singapore 189721, PH (065) 6256 6188; FAX (065) 6251 7188; email: Daniel.Bali@aurecongroup.com

ABSTRACT

After a section of the Nicoll Highway diaphragm wall (D-wall) construction collapsed in 2004, the Singapore authority require strutted D-wall designs to consider one strut failure (OSF) load cases – failure of a single strut or anchor at each construction stage. OSF is 3-dimensional (3D) and non-plane strain. It redistributes the lost strut load horizontally and vertically with arching effects. Rigorous OSF analyses would need 3D finite element method (OSF/3D FE), which takes huge amounts of computing time and memory space. Thus OSF is often analysed in 2-dimensional finite element (OSF/2D FE) models assuming either the whole layer of struts removed (WSF/2D) or their axial stiffness reduced. However, the soil-structure interaction is complex and the design bending moments (BM) and shears are often under-estimated. This paper presents a new and generic mathematical model to solve the OSF problem by applying the orthotropic plate bending theory (PB) to OSF/2D Plaxis models. Fictitious "rigidity factors" are introduced to solve the PB governing equations (eqn) and determine the strut loads, wall BMs and shears. The OSF/2D–PB model is then applied to the strutted D-wall design at Upper Changi Station, Singapore Downtown Line Stage 3 MRT extension Package C. This is a new railway line linking the Stage 1 Chinatown Station to airport with 9km tunnels and 6 stations each about 30m wide, 200m long and 30m underground. The results are compared with the OSF/3D Plaxis results. The OSF/2D–PB model and its benefits over the OSF/3D and the WSF/2D are discussed.

Keywords: one strut failure, Mindlin's plate, soil structure interaction, arching effect, rigidity factor

1 INTRODUCTION & BACKGROUND INFORMATION

Historically OSF studies are scarce. Strom et al. (2000) calculated pressures from OSF on a tieback wall by spreading the lost anchor force as triangularly distributed loads to adjacent supports, assuming the total lateral earth pressure being unaltered. This ignored the effects due to wall bending and shear stiffnesses and thus over-simplified the problem. Cheang et al. (2008) demonstrated rigorous OSF analyses by 3D Plaxis models. This paper applies the orthotropic plate bending theory (Mindlin, 1951 and Luo et al, 1995) to 2D FE soil-structure interaction analyses to reconstruct the OSF/3D results.

2 OSF/2D – PB MODEL

2.1 Assumptions and Mathematical Derivations

The model adopts the following assumptions:

a. The diaphragm wall (D-wall) is orthotropic and the orthotropic plate bending theory is applicable.
b. By using a reduced (say r %) axial stiffness for the lost strut, the OSF/2D FE model can simulate the OSF/3D wall horizontal deflection profile locally. The lost strut axial load F as determined by the OSF/2D model would spread horizontally and equally between the two struts adjacent to it.
c. The 2D FE model for the normal load case[1] with an additional axial load of ½F applied to the lost strut (which is modelled without any reduction in the axial stiffness in the normal load case) can locally simulate the OSF/3D wall deflection profile at the strut horizontally adjacent to the lost strut.
d. The effect of friction along the soil-wall interface on wall bending moment and shear is negligible.

[1] The normal load case is defined as the construction stage immediately before the one strut failure load case.

By Mindlin's plate theory for an orthotropic D-wall lying on the x-y plane with a lost strut at (0, 0),

the wall bending moment BM along the vertical y axis = $M_y = -D_{12}\frac{\partial \phi_x}{\partial x} - D_{11}\frac{\partial \phi_y}{\partial y}$; (1)

the horizontal shear along z-axis in the x-z plane = $V_y = -D_{12}\frac{\partial^2 \phi_x}{\partial y \partial x} - D_{33}\left(\frac{\partial^2 \phi_x}{\partial y \partial x} + \frac{\partial^2 \phi_y}{\partial x^2}\right) - D_{11}\frac{\partial^2 \phi_y}{\partial y^2}$; $(2a)$

the horizontal shear along z-axis in the y-z plane = $V_x = -D_{12}\frac{\partial^2 \phi_y}{\partial y \partial x} - D_{33}\left(\frac{\partial^2 \phi_y}{\partial y \partial x} + \frac{\partial^2 \phi_x}{\partial y^2}\right) - D_{22}\frac{\partial^2 \phi_x}{\partial x^2}$; $(2b)$

the total lateral earth pressure on wall = $q_{3D} = D_{22}\frac{\partial^3 \phi_x}{\partial x^3} + (D_{12} + 2D_{33})\left(\frac{\partial^3 \phi_x}{\partial y^2 \partial x} + \frac{\partial^3 \phi_y}{\partial y \partial x^2}\right) + D_{11}\frac{\partial^3 \phi_y}{\partial y^3}$; (3)

and also by shear strain formulation, $V_y = \kappa D_{44}\left(\frac{\partial w}{\partial y} - \emptyset_y\right)$ $(4a)$

$V_x = \kappa D_{55}\left(\frac{\partial w}{\partial x} - \emptyset_x\right)$ $(4b)$

and $q_{3D} = -\kappa D_{55}\left(\frac{\partial^2 w}{\partial x^2} - \frac{\partial \phi_x}{\partial x}\right) - \kappa D_{44}\left(\frac{\partial^2 w}{\partial y^2} - \frac{\partial \phi_y}{\partial y}\right)$ $(4c)$

where ϕ_x and ϕ_y are the angles between the z-axis and the normal to the middle plane of the wall cross section along the x and the y-axes respectively, κ = shear correction factor = 5/6, w = w(x, y) = the wall horizontal deflection; D_{ij} (i, j = 1 to 5) = wall elastic stiffnesses. Since the OSF/2D and the OSF/3D total lateral earth pressures on the wall are the same, we re-write eqn (3) for the boundary conditions at x=0 and x=S as follows: (suffixes 2D and 3D denote 2- and 3-dimensional cases respectively.)

$$q_{2D}(0,y) \equiv q_{3D}(0,y) = D_{22}\frac{\partial^3 \phi_x}{\partial x^3} + (D_{12} + 2D_{33})\left(\frac{\partial^3 \phi_x}{\partial y^2 \partial x} + \frac{\partial^3 \phi_y}{\partial y \partial x^2}\right) + D_{11}\frac{\partial^3 \phi_y}{\partial y^3}\Big|_{x=0} \quad ; \qquad (5)$$

$$q_{2D}(S,y) \equiv q_{3D}(S,y) = D_{22}\frac{\partial^3 \phi_x}{\partial x^3} + (D_{12} + 2D_{33})\left(\frac{\partial^3 \phi_x}{\partial y^2 \partial x} + \frac{\partial^3 \phi_y}{\partial y \partial x^2}\right) + D_{11}\frac{\partial^3 \phi_y}{\partial y^3}\Big|_{x=S} \quad . \qquad (6)$$

We neglect shear V_x in eqns (2b) and (4b) and put $\phi_x = \partial w/\partial x$ and $V_{y(3D)} \cong V_{y(2D)}$ since by symmetry $\phi_x = 0 = \partial w/\partial x$ at x=0 (i.e. pure bending along the x-axis) and the y-direction of D-walls is always more heavily reinforced than the horizontal x-direction, and the shear stiffness D_{55} of the y-z plane is very small compared with D_{44} of the x-z plane.

Hence from eqn (2a) $$V_x = -D_{12}\frac{\partial^2 \phi_y}{\partial y \partial x} - D_{33}\left(\frac{\partial^2 \phi_y}{\partial y \partial x} + \frac{\partial^2 \phi_x}{\partial y^2}\right) - D_{22}\frac{\partial^2 \phi_x}{\partial x^2} \cong 0. \qquad (7)$$

And from eqn (4c) $$q_{2D} = E_1 I\frac{\partial^3 \phi_y}{\partial y^3} \equiv q_{3D} \cong -\kappa D_{44}\left(\frac{\partial^2 w}{\partial y^2} - \frac{\partial \phi_y}{\partial y}\right) = q_{3D}{}^*, \qquad (8)$$

where $E_1\mathrm{I}$ is the wall flexural stiffness about the x-axis with plane strain condition in the x-direction. Now approximate w(x, y) near y=0 by a modified normal distribution eqn. (Peck,1969 and Chow,1994):

$$\mathrm{w(x,y)} = c\, e^{bx^2}\left(\frac{A + Bx^2}{A + Bx^2 + x^4}\right) + w(\infty, y) \qquad (9)$$

where

$$\mathrm{b} = -\frac{1}{S^2} log_e\left[\frac{w(0,y) - w(\infty,y)}{w(S,y) - w(\infty,y)}\left(\frac{A + BS^2}{A + BS^2 + S^4}\right)\right], \qquad (10)$$

$$\mathrm{c} = w(0,y) - w(\infty,y). \qquad (11)$$

S is the horizontal strut spacing. A and B are horizontal arching effect parameters such that the 4th derivative of the function w(x, y) with respect to (w.r.t.) x reduces at x=0 and increases at x=S. Thus the total lateral earth pressure q drops at the lost strut position and rises at the adjacent struts. By introducing a rigidity factor R to the wall stiffness $E_1\mathrm{I}$, we convert the OSF/2D bending moment M_y* to the OSF/3D M_y at y=0 as follows:

$$\mathrm{R}M_y^* = -\,\mathrm{R}\,E_1 I\,\frac{\partial \phi_y}{\partial y} = M_y = -D_{12}\frac{\partial \phi_x}{\partial x} - D_{11}\frac{\partial \phi_y}{\partial y}\ . \qquad (12)$$

As $\partial\phi_x/\partial x$ contains an e^{bx^2} term and M_y is symmetric w.r.t. x, by inspection we can put $\mathrm{R} = \sum_{n=1}^{\infty}\xi(1 + \lambda_n x^{2n})e^{bx^2}$, where ξ and λ_n are parameters independent of x. As a first approximation we have R= $\xi(1 + \lambda x^2)e^{bx^2}$, with parameters ξ and λ determined by $\partial\phi_x/\partial x$ and $\partial\phi_y/\partial y$ at x=0 and x=S respectively.

2.2 Methodology to determine Diaphragm Wall Bending Moments and Shears

A 2D FE analysis (named as Analysis No.1) is carried out for the normal load case to obtain w(∞, y). The analysis then adopts a reduced lost strut stiffness of r % to determine F, q_{2D} and the OSF/2D w,

$\partial w/\partial y$, $\partial^2 w/\partial y^2$, $\partial^3 w/\partial y^3$, $\partial^4 w/\partial y^4$ and also $\partial\phi_y/\partial y$, $\partial^2\phi_y/\partial y^2$, $\partial^3\phi_y/\partial y^3$ at x=0 by putting $D_{11}= E_1 I$ and all the derivatives w.r.t. x equal to zero in eqns (1), (2a) and (3). Another 2D FE analysis (Analysis No.2) is performed for the normal load case with ½F added to the strut load at y=0 to determine q_{2D}, w, $\partial w/\partial y$, $\partial^2 w/\partial y^2$, $\partial^3 w/\partial y^3$, $\partial^4 w/\partial y^4$and also $\partial\phi_y/\partial y$, $\partial^2\phi_y/\partial y^2$, $\partial^3\phi_y/\partial y^3$. By assumptions (b) and (c) we adopt the results from Analysis Nos. 1 and 2 as the 3D case values at the lost strut position (0, 0) and the adjacent strut (S, 0) respectively. By differentiating eqn (9) w.r.t. x and y and eqns (7), (12) w.r.t. x, derivatives of w (i.e. $\partial w/\partial x$, $\partial^2 w/\partial x^2$, $\partial^3 w/\partial x^3$, $\partial^3 w/\partial y\partial x^2$, $\partial^3 w/\partial x\partial y^2$, $\partial^4 w/\partial y^2\partial x^2$and $\partial^4 w/\partial x^4$) and ϕ_y (i.e. $\partial^3\phi_y/\partial y\partial x^2$and $\partial^2\phi_y/\partial x\partial y$) at (0, 0) and (S, 0) can be expressed in terms of A and B. Since q_{3D} is maximum at x=S, we have from eqn (8):

$$\frac{\partial q_{3D}}{\partial x} = -\kappa D_{44}\left(\frac{\partial^3 w}{\partial y^2 \partial x} - \frac{\partial^2 \emptyset_y}{\partial x \partial y}\right)\Big|_{x=S} = 0. \qquad (13)$$

Hence eqns (5), (6) and (13) can be reduced to 3 simultaneous equations in 3 unknowns: r, A, B. Now Analysis Nos. 1 and 2 are repeated for a range of values of r to get the wall deflection w, rotation ϕ_y and their derivatives at (0, 0) and (S, 0). By assumptions (b) and (c) these are taken as the 3D case values to calculate the following variables, namely q_{3D}(0, 0) in eqn (5), q_{3D}(S, 0) in eqn (6) and $\partial q_{3D}/\partial x$ at (S, 0) in eqn (13). They are then plotted with the corresponding q_{2D} values against r for an iterative graphic solution of r, A, B. These values of r, A and B are then used in eqns (9), (1) and (2a) to obtain M_y and V_y at the lost strut position (0, 0) and the adjacent strut (S, 0). For the strut at a distance H directly above or below the lost strut, the following wall deflection profile near y = H is assumed.

$$\mathrm{w(x,y)} = \{w(0,y) - w(\infty,y)\}e^{b'x^2}\left[\frac{A'}{A' + B'x^2 + x^4}\right]^{0.5} + w(\infty,y) \qquad (14)$$

where

$$\mathrm{b'} = -\frac{1}{S^2} log_e\left[\frac{w(0,y) - w(\infty,y)}{w(S,y) - w(\infty,y)}\left(\frac{A'}{A' + B'S^2 + S^4}\right)^{0.5}\right], \qquad (15)$$

A' and B' are unknown constants. By eqn (14) derivatives of w(x, y) w.r.t. x and y at (0, H) and (S, H) can be found. The BM and shear at strut level (0, H) are evaluated by repeating the above procedures and solving r, A', B' at (0, H).

2.3 OSF/2D – PB Model Analysis for Upper Changi Station (UPC) Diaphragm Wall Design

UPC Station is located at Upper Changi Road East, Singapore. It is a reinforced concrete box structure about 183m long by 26m wide constructed within permanent D-walls of 1.2m thick. Bottom-up construction method with 6 layers of steel strut (S1 to S6) was adopted. The excavation is about 30m below ground. The site geology comprises about 3m thick fill over-lying successive layers of old alluvium soil of types OD to OA with the design groundwater table on the ground surface as shown in Figure 1. A live load (L.L.) of 23kPa is applied on the ground level. The design geotechnical parameters and D-wall parameters are shown in Tables 1, 2, 3 and 4 respectively.

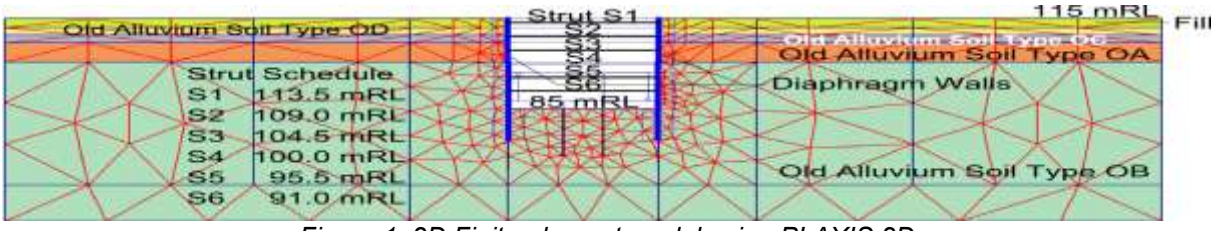

Figure 1. 2D Finite element model using PLAXIS 2D

Table 1: Adopted design geotechnical parameters

Soil	Unit weight [kN/m^3]	Total stress [kPa]		Effective stress			† Coeff. of At-rest earth pressure,K_o	Permeability [m/s]	R^*_{inter}
		Peak undrained shear strength, S_u	Elastic modulus,E_u	Cohesion c' [kPa]	Friction angle ϕ'	Poisson's ratio**, ν			
Fill	20	30	10,000	1	28°	0.3	1	10^{-6}	0.5
OD	20	130	52,000	1	30°	0.3	1	10^{-7}	0.5
OC	21	235	94,000	10	32°	0.3	1	10^{-7}	0.5
OB	21	250	120,000	20	35°	0.3	1	10^{-7}	0.5
OA	21	250	150,000	25	35°	0.3	1	10^{-7}	0.5

*R_{inter}= strength reduction factor along soil-wall interface.
**Poisson's ratios refer to the drained conditions.
†From past experience with fill and Types OA to OD soils in Singapore, K_o= 1is adopted for initializing horizontal soil stresses in Plaxis. Subsequent Plaxis plastic calculations would adopt "undrained effective stress analyses" with ν=0.3 and the drained elastic moduli.

Table 2. Waler section elastic modulus E, stiffness $E_s I_w/H$ parameters for OSF/2D-PB model

$E = 2x10^8$kPa	Waler W1	Waler W2	Waler W3	Waler W4	Waler W5	Waler W6
$E_s I_w/H$	0.56	0.98	0.98	1.02	0.8	0.89

Table 3: Diaphragm wall and steel strut parameters for OSF/2D Plaxis analysis

Wall unit weight γ (kN/m^3)	Wall E_1 [GPa]	ν	Wall thickness h [m]	Strut Axial Stiffness EA [kN]					
				Strut length L = 26m, Strut horizontal spacing S = 6m					
				Strut S1	Strut S2	Strut S3	Strut S4	Strut S5	Strut S6
6	28	0.2	1.2	12,400,000	21,100,000	21,100,000	23,200,000	15,600,000	19,000,000

*Table 4: Diaphragm wall parameters for OSF/2D-PB model**

Wall elastic modulus [GPa]		Poisson's ratio, ν		D_{11} $\Updownarrow$ $\frac{E_1 h^3}{12(1-\nu_{12}\nu_{21})}$ [GPa.m^4/m]	D_{12} $\Updownarrow$ $\frac{\nu_{21} E_2 h^3}{12(1-\nu_{12}\nu_{21})}$ [GPa.m^4/m]	D_{22} $\Updownarrow$ $\frac{E_2 h^3}{12(1-\nu_{12}\nu_{21})}$ [GPa.m^4/m]	D_{33} $\Updownarrow$ $\frac{E_1 h^3}{24(1+\nu_{12})}$ [GPa.m^4/m]	D_{44} $\Updownarrow$ $\frac{G_{13} h}{2}$ [GPa]	D_{55} $\Updownarrow$ $\frac{G_{12} h}{2}$ [GPa]
E_1	E_2 (waler included)	ν_{12}	$\nu_{21} = \nu_{12}\frac{E_1}{E_2}$						
28	7.35 at S3 7.66 at S4	0.2	0.76 at S3 0.73 at S4	4.76 at S3 4.72 at S4	0.95 at S3 0.94 at S4	1.25 at S3 1.29 at S4	1.68	8.4	0.086

* Suffix 1 denotes the vertical y-axis, 2 denotes the horizontal x-axis, 3 denotes the horizontal z-axis

The Plaxis analysis adopted the undrained Mohr-Coulomb model which simplified the soil non-linear stress-dependent stress-strain behaviour to elastic-perfectly plastic and simulated the undrained behaviour with undrained effective stress analysis using undrained strength parameters (Plaxis BV, 2011). It also modelled the D-walls as Mindlin plates. As the D-wall span-depth ratio at OSF is about 10, the OSF-PB analysis for Strut S4 adopted thin-plate formulation by taking $\partial w/\partial y = \phi_y$, ignoring eqns (4a) to (4c) in Section 2.1 and solving $\partial V_x/\partial x = 0$ at x=0; whilst analysis for Strut S3 adopted the Mindlin plate formulation. Staged construction modelling followed Table 5.

Table 5. Staged construction modelling

Phase no.	Activity	Phase no.	Activity	Phase no.	Activity
1	Install Wall & L.L.23kPa (0)*	6	Excavate to S3 (5)	11	Install S5 (10)
2	Excavate to S1 (1)	7	Install S3 (6)	12	Excavate to S6 (11)
3	Install S1 (2)	8	Excavate to S4 (7)	13	Install S6 (12)
4	Excavate to S2 (3)	9	Install S4 (8)	14	Excavate to 85mRL (13)
5	Install S2 (4)	10	Excavate to S5 (9)	15	OSF at S4 (14)

* The figure shown in bracket indicates the Phase no. from which the activity starts. Phase 0 is the initialization of soil stresses.

3 THREE DIMENSIONAL FINITE ELEMENT ANALYSIS FOR OSF BY PLAXIS 3D FE MODEL

An OSF/3D FE analysis was performed using PLAXIS 3D Foundation. The 3D FE model is 80m long, 36m wide, 70m high and cuboid-shaped. Basically it has five elements, namely the volume element, plate element, beam element, fixed-end anchor element and interface element (see Figure 2).

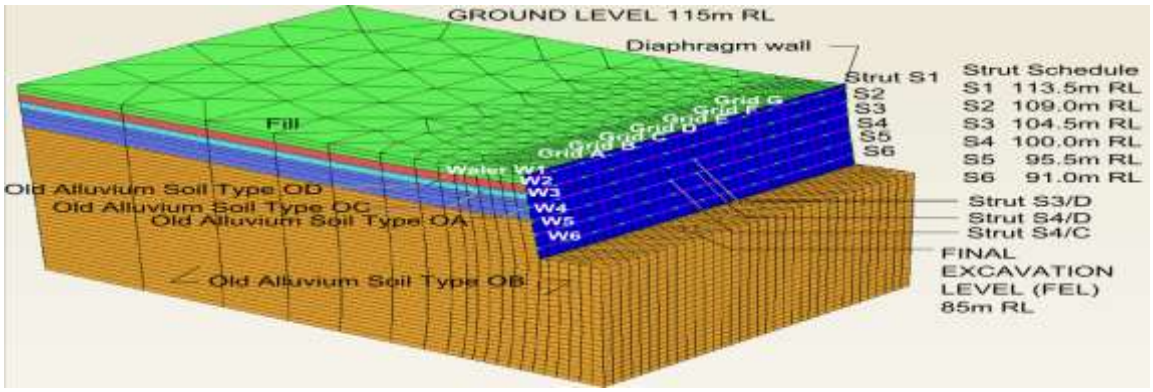

Figure 2. 3D Finite element model using PLAXIS 3D Foundation

A total 3632 pieces of 15-noded wedge volume elements were used in the model to represent the soil mass. The undrained Mohr-Coulomb model with soil parameters shown in Table 1 was adopted. Steel struts and walers were modelled as fixed-end anchor elements and beam elements respectively with input parameters given in Tables 6 and 7. The non-isotropic diaphragm walls were modelled by 8-noded quadrilateral Mindlin plate elements with directional stiffnesses. The horizontal direction elastic modulus was assumed to be 1/50 of that over the vertical direction (see Table 8). The interaction between the soil and the D-wall was simulated by interface elements with a reduction factor of 0.5. Standard boundary conditions were applied to the model.

Table 6. Strut axial stiffness (EA/L) parameters

	Strut S1	Strut S2	Strut S3	Strut S4	Strut S5	Strut S6
EA/L [kN/m]	9.55 x10^5	1.63 x10^6	1.63 x10^6	1.79 x10^6	1.20 x10^6	1.46 x10^6

Table 7. Waler section elastic modulus E, area A and area moment of inertia I parameters

E = 2x10^8kN/m^2	Waler W1	Waler W2	Waler W3	Waler W4	Waler W5	Waler W6
Area A [m^2]	0.088	0.147	0.147	0.149	0.121	0.133
I_2, (I_3) [x10^{-4}m^4]	125, (3.896)	220, (7.292)	220, (7.292)	230, (1.46)	180, (5.716)	200, (6.416)

* Suffix 1 denotes the vertical y-axis, 2 denotes the horizontal x-axis, 3 denotes the horizontal z-axis

Table 8. Diaphragm wall parameters for elastic modulus E and shear modulus G

	γ [kN/m^3]	E_1 [kN/m^2]	E_2 [kN/m^2]	ν_{12} [-]	G_{12}[kN/m^2]	G_{13}[kN/m^2]	G_{23}[kN/m^2]
D-wall	6	2.8 x10^7	5.6 x10^5	0.2	1.434 x10^5	1.4 x10^7	2.8 x10^5

* Suffix 1 denotes the vertical y-axis, 2 denotes the horizontal x-axis, 13 denotes "along the horizontal z-axis in the 'x-z 'plane"

A complete construction staging calculation followed Table 5. The OSF load case was simulated by de-activating only one strut - S4/D (see Figure 2) after the final excavation level (FEL) was reached. Due to its huge size, data input and subsequent execution of the Plaxis 3D analysis often took more than 24 hours (i.e. overnight) for each OSF load case.

4 SUMMARY & DISCUSSION OF OSF/2D-PB, WSF, OSF/2D & OSF/3D ANALYSIS RESULTS

4.1 Iterative Graphic Solutions for OSF/2D-PB Analysis

An iterative solution following the methodology in Section 2 for the lost strut S4/D is obtained in Figures 3, 4 and 5. The solution for strut S3/D is shown in Figures 6, 7 and 8.

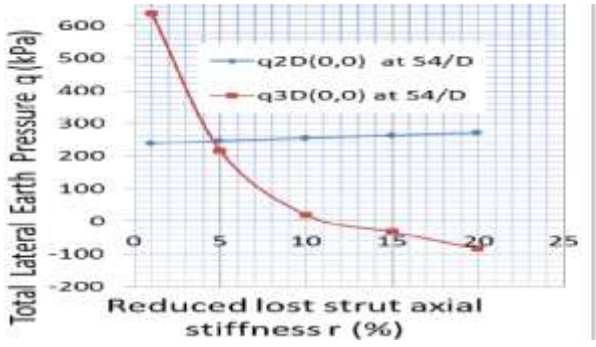

Figure 3. q at Strut S4/D

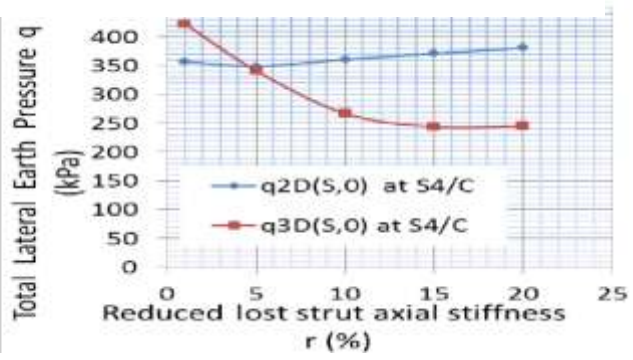

Figure 4. q at Strut S4/C

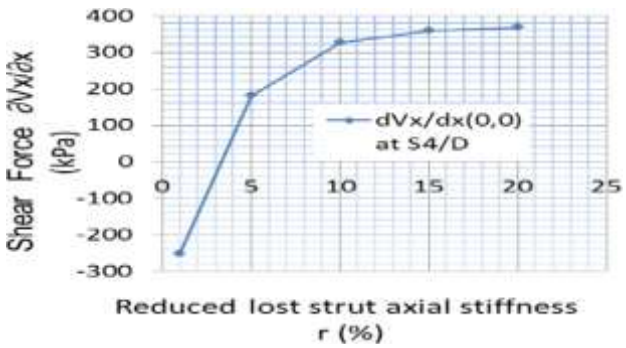

Figure 5. $\left.\frac{\partial V_x}{\partial x}\right|_{(0,0)}$ at Strut S4/D

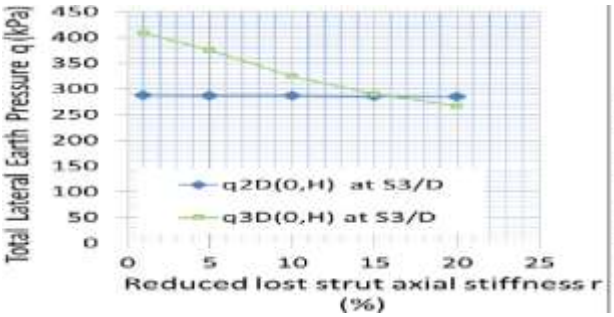

Figure 6. q at Strut S3/D

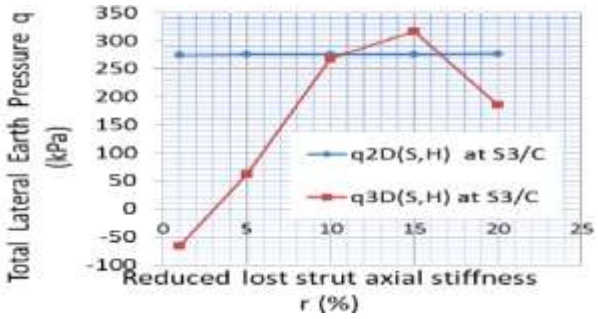

Figure 7. q at Strut S3/C

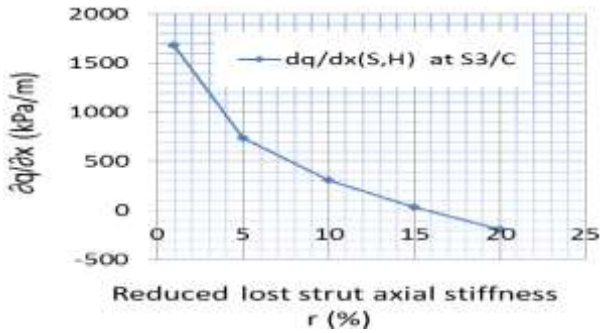

Figure 8. $\left.\frac{\partial q}{\partial x}\right|_{(S,H)}$ at Strut S3/C

Results of the OSF/2D-PB analysis are summarized in Table 9.

Table 9. Summary of OSF/2D-PB analysis results

Strut Position	b [m $^{-2}$]	c [m]	F [kN/m]	ξ [-]	λ [m $^{-2}$]	r	A[m^4]	B[m^2]
S4/D	-0.0436	0.00532	152	NA	NA	4.8%	324.0	1.75
S3/D	-0.00184	0.00187	444	1.44	-0.00184	16%	39.5	-7.70

4.2 Summary of OSF/3D, OSF/2D, WSF/2D & OSF/2D-PB Analysis Results

The D-wall horizontal deflections, BMs, shears and strut loads for the normal and the OSF load cases from the Plaxis 2D, 3D and 2D-PB analyses are presented in Figure 9 and Table 10 respectively.

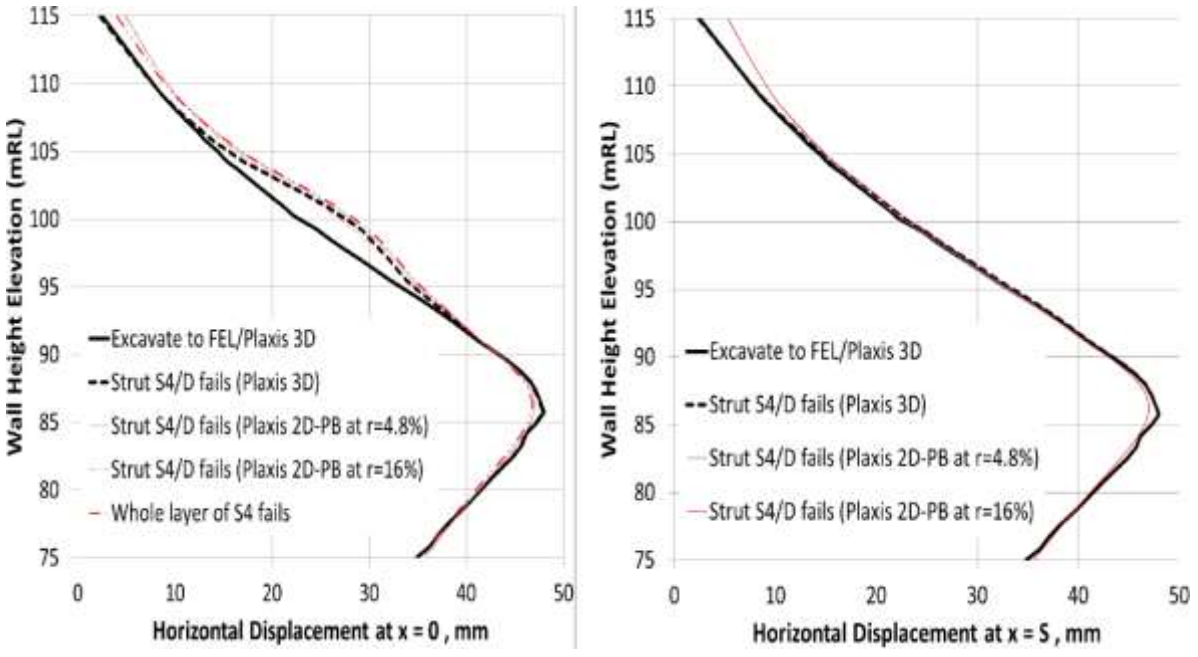

Figure 9. Wall horizontal deflection

Table 10. Summary of analysis results

Plaxis	Analysis results at strut location S4/D							Analysis results at strut location S3/D						
Model/Load case	r %	w mm	M_y kNm/m	V_y kN/m	V_x kN/m	q kPa	N_1[(1)] kN	r %	w mm	M_y kNm/m	V_y kN/m	V_x kN/m	q kPa	N_2[(1)] kN
3D/normal	100	22.8	-1096	-1112	-30.1	319	9389	100	15.0	-963	-755	-18.5	283	7120
3D/OSF	0	27.6 (22.8)	1589 (-1151)[(2)]	-66.5 (-1171)	-2.4 (-29.3)	247 (350)	10020	0	16.5	-1993	-1013	-25.8	300	9513
2D/normal	100	22.7	-1060	-922	unable to predict (NP)	314	9522	100	15.3	-1024	-702	unable to predict (NP)	278	6965
2D/WSF	0	28.5	1236	70.8		234	NP	0	17.9	-1486	-1183		284	11164
2D/OSF	5	28.0	1027	-5.7		247	NP	5	17.7	-1410	-1120		287	10783
2D-PB/OSF	4.8	28.1 (23.0)	1698 (-1117)	-50.1 (-1145)		246 (348)	10069	16	17.3	-1906	-1036		286	10067

(1) N_1= axial load at strut S4/C (horizontally adjacent to strut S4/D); N_2= axial load at strut S3/D (immediately above strut S4/D).
(2) Values shown in brackets indicate the respective values of wall deflection, BM, V and q at strut S4/C

4.3 Discussions on OSF/3D, OSF/2D, WSF/2D & OSF/2D-PB Analysis Results

The Plaxis 3D results in Figure 9 and Table 10 show that after OSF the horizontal deflection at the failed strut position (RL100m) increases greatly from 22.8mm to 27.6mm and that the wall BM changed from hogging to sagging with significant horizontal arching effects on the total lateral earth pressure at the lost strut level. However, the difference in wall deflections between the OSF/2D-PB and the OSF/3D Plaxis analyses at Strut S3 (and also S4) is within 1mm only. Shear V_x is also small. Hence V_x is negligible and assumptions (b) and (c) are justified. Table 10 also shows that the critical wall BMs, shears and strut axial loads predicted by the OSF/2D-PB and the OSF/3D Plaxis models are within ±7% of each other. Thus the adopted OSF/2D-PB model plate bending formulations match well with the Plaxis Mindlin plate element, and the assumed shear effects on bending are justified in this case. On the contrary, the OSF/2D and the WSF/2D analyses not only fail to predict the strut loads adjacent to the lost strut, but also under-estimate the wall BMs considerably by about 25 to 35%.

5 CONCLUSION

The OSF/2D-PB model has successfully captured the soil-structure interaction behaviour as well as the horizontal arching effect along the lost strut level. The model can predict the critical bending moments, shears and axial loads sufficiently close to the OSF/3D Plaxis model for practical design purposes. It is also more efficient and economical than the Plaxis 3D model which would require tremendous amounts of computing time and memory space. The study also reveals that the OSF/2D and the WSF/2D models always under-estimate the critical bending moments significantly and hence are not conservative for the OSF load case analysis.

6 ACKNOWLEDGEMENTS

The authors would like to thank Aurecon Singapore Ltd. for their supports for OSF numerical analyses.

REFERENCES

Cheang, W.L. et al. (2008) “Computational Geomechanics in Routine Geotechnical Analysis – The Plaxis Approach.” Plaxis Seminar, Lecture 1, Kuching 2008, Malaysia.

Chow, L. (1994). “Prediction of Surface Settlements due to Tunnelling in Soft Ground.” Brasenose College, University of Oxford.

Luo S., Suhling J.C. and Laufenberg T.L. (1995). “Bending and Twisting Tests for Measurement of the Stiffnesses of Corrugated Board” AMD-VOL. 209/MD-Vol.60, Mechanics of Cellulosic Materials, ASME 1995.

Mindlin, R.D. (1951). “Influence of Rotatory Inertia and Shear on Flexural Motions of Isotropic Elastic Plates.” ASME Journal of Applied Mechanics, Volume 18, pp. 31-38.

Peck, R.B. (1969). “Deep excavations and tunnelling in soft ground.” Proceedings of 7th International Conference of Soil Mechanics and Foundation Engineering, State of the Art, pp. 226-290.

Plaxis BV (2007). “Plaxis 3D Foundation, Version 2”. Delft, the Netherlands.

Plaxis BV (2011). “Plaxis 2D 2010”. Delft, the Netherlands.

Strom R. W. and Ebeling R. M. (2000) “Method Used in Tieback Wall Design and Construction to Prevent Local Anchor Failure, Progressive Anchorage Failure, and Ground Mass Stability Failure”, US Army Corps of Engineers, Chapter 4.

Timoshenko, S. (1959). “Theory of Plates and Shells”. McGraw Hill, 2nd Edition, Art.39, pp.165-173.